Conformer selection and differential restriction of ligand mobility by a plant lectin

Conformational behaviour of Galβ1-3GlcNAcβ1-R, Galβ1-3GalNAcβ1-R and Galβ1-2Galβ1-R′ in the free state and complexed with galactoside-specific mistletoe lectin as revealed by random-walk and conformational-clustering molecular-mechanics calculations, molecular-dynamics simulations and nuclear Overhauser experiments

Martine GILLERON [1,2], Hans-Christian SIEBERT [1,3], Herbert KALTNER [3], Claus-Wilhelm VON DER LIETH [4], Tibor KOZÁR [4,5,7], Koen M. HALKES [1], Elena Y. KORCHAGINA [6], Nicolai V. BOVIN [6], Hans-Joachim GABIUS [3] and Johannes F. G. VLIEGENTHART [1]

[1] Bijvoet Center for Biomolecular Research, Department of Bio-Organic Chemistry, Utrecht University, The Netherlands
[2] Institut de Pharmacologie et de Biologie Structurale du CNRS, Toulouse, France
[3] Institut für Physiologische Chemie, Tierärztliche Fakultät, Ludwig-Maximilians-Universität, München, Germany
[4] Deutsches Krebsforschungszentrum, Zentrale Spektroskopie, Heidelberg, Germany
[5] GlycoDesign Inc., Toronto, Canada
[6] Shemyakin Institute of Bioorganic Chemistry, Russian Academy of Sciences, Moscow, Russia
[7] Institute of Experimental Physics, Slovak University of Sciences, Kosice, Slovak Republic

To study conformational parameters of ligands before and after complex formation with the galactoside-binding agglutinin of *Viscum album* L. (VAA) in solution, combined computer-assisted random walk molecular mechanics (RAMM) calculations extended by conformational clustering analysis (CCA), molecular dynamics (MD) simulations as well as two-dimensional rotating-frame nuclear Overhauser effect (ROE) and two-dimensional nuclear Overhauser effect (NOE) spectroscopy NMR experiments were employed. Derivatives of the naturally occurring disaccharides Galβ1-3GlcNAcβ1-R and Galβ1-3GalNAcβ1-R as well as of a synthetic high-affinity binding partner, i.e. the disaccharide Galβ1-2Galβ1-R′, were chosen as ligands in this study. The disaccharides displayed inherent flexibility in the valley of the global minimum between Φ/Ψ combinations of (40°/60°) and (40°/−60°). Calculations of the de-N-acetylated sugars revealed that presence of this group did not markedly influence the distribution of low-energy conformers in the Φ, Ψ, E plot. Occupation of side minima at Φ/Ψ (180°/0°) or (0°/180°) is either unlikely or low according to the results of MD simulations and RAMM calculations extended by CCA. Notably, these side minima define conformations which are not stable during a MD simulation. Transitions to other minima occur already a few picoseconds after the start of the simulation. NMR experiments of the free-state ligand confirmed the validity of the data sets obtained by the calculations. Following the description of the conformational space in the free-state NMR experiments were performed for these disaccharides complexed with VAA. They yielded two interresidual contacts for Galβ1-3GlcNAcβ1-R and Galβ1-2Galβ1-R′. The ligand conformations in the complex did not deviate markedly from those of a minimum conformation in the free state. One- and two-dimensional transferred nuclear Overhauser enhancement (TRNOE) experiments at different mixing times excluded the influence of spin-diffusion effects. When the NOE build-up curves in the three studied cases were compared, the residual mobility of the penultimate carbohydrate unit of Galβ1-3GalNAcβ1-R was observed to be higher than that of the respective hexopyranose unit of the other two bound ligands. Due to the availability of the conformational parameters of Galβ1-2Galβ1-R′ in association with a galectin, namely the β-galactoside-binding protein from chicken liver, it is remarkable to note that this ligand displays different conformations in the binding sites of either the plant or the animal lectin. They correspond to local energy-minimum conformations in the Φ, Ψ, E plot and substantiate differential conformer selection by these two lectins with identical nominal monosaccharide specificity.

Keywords: lectin; agglutinin; conformational analysis; nuclear Overhauser effect; molecular modelling.

Carbohydrate-protein recognition plays essential roles in many biological processes such as cell recognition, intercellular adhesion and growth regulation [1−3]. To trigger any physiological response, a receptor such as a lectin must specifically associate with a carbohydrate ligand whose structural features in solution will enable a variety of primarily enthalpically favourable interactions involving hydrogen bonds and hydrophobic stacking [4−10]. To comprehend the molecular details of the interaction process in solution, conformational aspects of the carbohydrate ligand are amenable to thorough calculations and experimental scrutiny. In principle, it is possible that a conformational adaptation is required to generate a snug fit between functional groups of the protein and the sugar ligand in the carbohydrate recognition domain or that the global-minimum conformation itself presents the appropriate spatial parameters. This study, employing RAMM calculations extended by CCA, MD simulations and NMR measurements, is designed to address this question for a plant lectin with immunomodulatory potency.

The galactoside-binding lectin of mistletoe (*Viscum album* L. agglutinin, VAA) belongs to the group of AB-type plant toxins [11, 12]. It consists of two disulfide-bridge-linked subunits, a carbohydrate-specific B-chain which binds to cell surfaces and is presumed to facilitate entry of the toxin into the cell, and a toxic A-chain, which inhibits protein synthesis by its activity as site-specific rRNA N-glycosidase. Following galactoside-dependent binding and ensuing signalling, several cellular responses such as secretion of cytokines, namely tumor necrosis factor-α, interleukin-1 and interleukin-6 by human peripheral blood mononuclear cells, can be measured in the non-toxic dose range of $5−50$ ng/ml$\times 10^6$ cells *in vitro*, warranting thorough examination of the potency of tumor inhibition or stimulation in preclinical model studies [2, 13−15]. The capacity of the lectin to act as a biological response modifier has prompted the study of its carbohydrate specificity with saccharides, cluster glycosides, and neoglycoproteins and of its cross-linking capacity with asialofetuin [16−18]. The application of this panel of probes revealed primarily recognition of the terminal galactose unit irrespective of the anomeric linkage with further importance of the equatorial hydroxyl group of the penultimate saccharide residue that is located next to the glycosidic linkage. Having defined the chemical constitution of suitable ligands from a panel of (synthetic) test substances, the next step is to assess the conformational parameters of a ligand in association with the lectin.

To address this question for receptor-ligand complexes in solution, MM- and MD-supported NMR spectroscopy has been established as a powerful tool to derive conformations from time- and ensemble-averaged data sets. When a ligand exchanges rapidly within the time scale of spin-lattice relaxation between the solution and its binding site in a receptor, the TRNOE experiment is a valuable approach for determination of receptor-bound ligand features in solution [19−23]. This experiment takes advantage of the transfer of information about the bound state to the free state involving measurement of a negative NOE and has already been instrumental in inferring information on conformation as well as exchange dynamics of carbohydrates bound to their cognate lectin or antibody (for reviews, see [10, 24−26]). Since protein and oligosaccharide come into intimate contact, it is probable that the association can involve conformer selection, alteration of parameters of the free state and/or restrictions of the conformational freedom [4−10]. Presently, no evident rules are discerned that allow predictions of the mode of influence for an individual lectin. To extend our level of knowledge in this field, we have performed the study described here.

Three ligands with different binding affinities for VAA were chosen, i.e. Galβ1-3GlcNAcβ1-R, Galβ1-3GalNAcβ1-R and Galβ1-2Galβ1-R', for the interaction studies (R = OCH$_2$CHCH$_2$,

R' = O(CH$_2$)$_3$NHCOCF$_3$). Additionally, computer calculations on two related, i.e. the de-N-acetylated disaccharides (Galβ1-3Galβ1-R and Galβ1-3Glc1-R) were included in order to assess the impact of presence of the 2'-N-acetyl group on the conformational behaviour of the two physiological disaccharides. The combination of RAMM calculations extended by the CCA approach, MD simulations with different values of the dielectric constant ε or explicit consideration of the solvent molecules as well as NMR techniques yielded a comparison between the free-state conformations and those of the bound state for the tested ligands. The results indicate that a conformation at least very similar to an energy minimum of the free state appeared to be adopted in the complex, excluding any major alteration of a low-energy ligand conformation upon binding, and that only the penultimate sugar unit of Galβ1-3GalNAcβ1-R maintained a rather high mobility after complex formation.

MATERIALS AND METHODS

Materials. VAA and its carbohydrate-binding B subunit were purified from extracts of commercially available dried leaves, as described previously [14]. Galβ1-3GlcNAcβ1-R, Galβ1-3GalNAcβ1-R and Galβ1-2Galβ1-R' were synthesised, as described elsewhere [27, 28].

Molecular dynamics simulations and random walk molecular mechanics calculations extended by a conformational clustering analysis. Molecular modelling calculations were performed using various SGI and IBM workstations and PCs as platforms. The initial geometry of the disaccharides was either generated applying the WWW version of the program SWEET [29] or with the aid of the CARBOHYDRATE option of the BIOPOLYMER module of INSIGHTII. Charges and atom types were assigned with the automatic parameter and atomic charge assignment procedure of INSIGHTII. Additionally, the parametrisation for the CHEAT (carbohydrate hydroxyls represented by extended atoms) force field [30] was also implemented into the standard MSI/Biosym environment. MD simulations at a constant temperature ($T = 300$ K or 400 K) were performed. Three different values for the dielectric constant were selected in MD simulations, namely $\varepsilon = 1$, $\varepsilon = 4$ and $\varepsilon = 80$, to account for an implicit influence of water. Moreover, solvent molecules were deliberately incorporated as an explicit part of the simulation procedure. No additional forces or cut-off parameters were taken into consideration. The distance-dependent value of the dielectric constant was also considered in order to properly describe the intramolecular hydrogen bonding of the studied molecules. An integration-time step of 1 fs was used for all simulations. The ANALYSIS module of INSIGHTII was applied to monitor the various trajectories within MD simulations.

In addition to MD simulations with the CVFF (consistence valence force field) [31, 32] calculations with CHEAT [30], AMBER (assisted model building with energy refinement) [33, 34], CHARMM (chemistry at Harvard macromolecular mechanics) [35] and GROMOS (Groningen molecular simulations) [36] force fields were also performed to disclose any conformational preference within the energy potential description of the structure of the disaccharides. Explicit inclusion of water molecules was restricted to the use of the CVFF or GROMOS force fields within the simulations.

The RAMM method [37, 38] which is based on the MM2-87 [39, 40] force field yielded a description of the relaxed conformational energy surfaces for grid-point-defined rotations around the torsion angles Φ, Ψ of the glycosidic bond. The effect of variations of the dielectric constant on the shape of the conformational energy surface was also analysed. Similar to the

MD simulations, three values of the dielectric constant, namely $\varepsilon = 1.5$, $\varepsilon = 4$ and $\varepsilon = 80$, were independently applied in the calculation of the electrostatic energy contribution. No explicit solvent molecules were considered during this type of conformational analysis.

Whereas at this stage of the calculations internal parameters of each carbohydrate unit of the disaccharides (i.e. ring geometry and pendant groups) had been obtained, it is essential to remember the remaining constraints imposed on the Φ/Ψ torsion angles by the definition of the grid. This factor can lead to an actual shift of the positions of minima in the fixed coordinate system. In the worst case, it is responsible for a lack of detection of actual minimum positions which are not located in the immediate vicinity of grid points. Therefore, the standard RAMM protocol was extended by the CCA approach [41]. Having released the remaining constraints for any starting position, the Φ/Ψ torsion angles will undergo changes aiming at achieving a low-energy position. These adaptations in the molecular mechanics calculations are equivalent to the motions of balls in a hilly countryside. Like pathfinders they will exploit any suitable downhill route to end up in clusters of low-altitude destinations, explaining the name of the approach. Following a final reoptimisation of the internal geometric parameters the results of this refinement to the RAMM protocol are conveniently depicted in the Φ/Ψ plot. These calculations were performed for all studied disaccharide derivatives, i.e. Galβ1-3GlcNAcβ1-R, Galβ1-3Gal-NAcβ1-R, Galβ1-3Glcβ1-R, Galβ1-3Galβ1-R and Galβ1-2Galβ1-R$'$.

NMR spectroscopy. 360-MHz and 500-MHz ^{1}H-NMR spectra of the free disaccharide derivatives or disaccharide-lectin complexes were recorded at 298 K or 300 K on Bruker AM 360 and Bruker AMX 500 spectrometers, respectively, at the Bijvoet Center, Department of NMR Spectroscopy, Utrecht University and at the *Institut de Pharmacologie et de Biologie Structurale du CNRS*, Toulouse. Chemical shifts are expressed relative to the internal signal of acetone at 2.225 ppm. Disaccharides and disaccharide-lectin complexes were measured in 99.96 atom % D$_2$O (MSD Isotopes). The pD value, which is correlated to the pH value by the relation pD = pH$_{meter\ reading}$ + 0.4, was usually set to a value of 7. The chemical shifts were assigned by two-dimensional (2D) COSY, RCT and HMQC-NMR experiments. Mixing times of 25 ms, 50 ms, 75 ms and 100 ms were applied when the disaccharide-VAA complex was analysed by NOE experiments. ROE experiments were performed under nearly identical conditions to obtain information about the free-state conformations of the studied disaccharides and the influence of spin diffusion in the complex [42]. NOE spectra of the free disaccharide ligands were recorded at mixing times of 75 ms, 150 ms, 250 ms and 350 ms. Build-up curves were established from NOE spectra of free and complexed ligands.

RESULTS

MM and MD calculations of the disaccharides. The solution conformations of the disaccharides were inferred from RAMM calculations combined with the CCA approach and MD simulations. RAMM calculations of Galβ1-3GlcNAcβ1-R in which Φ and Ψ angles were varied in steps of 10° indicated the presence of five energy minima below an energy level of 20.93 kJ/mol (5 kcal/mol): $(\Phi/\Psi) = (30°/15°)$, $(20°/-50°)$, $(60°/60°)$, $(20°/180°)$ and $(180°/0°)$ at the dielectric constant of water ($\varepsilon = 80$), reduction of this value only revealing a minor impact (Fig. 1). Conformational clustering data for Galβ1-3GlcNAcβ1-R considering two different dielectric constants allowed a refined delineation of the conformational space of this disaccharide. After
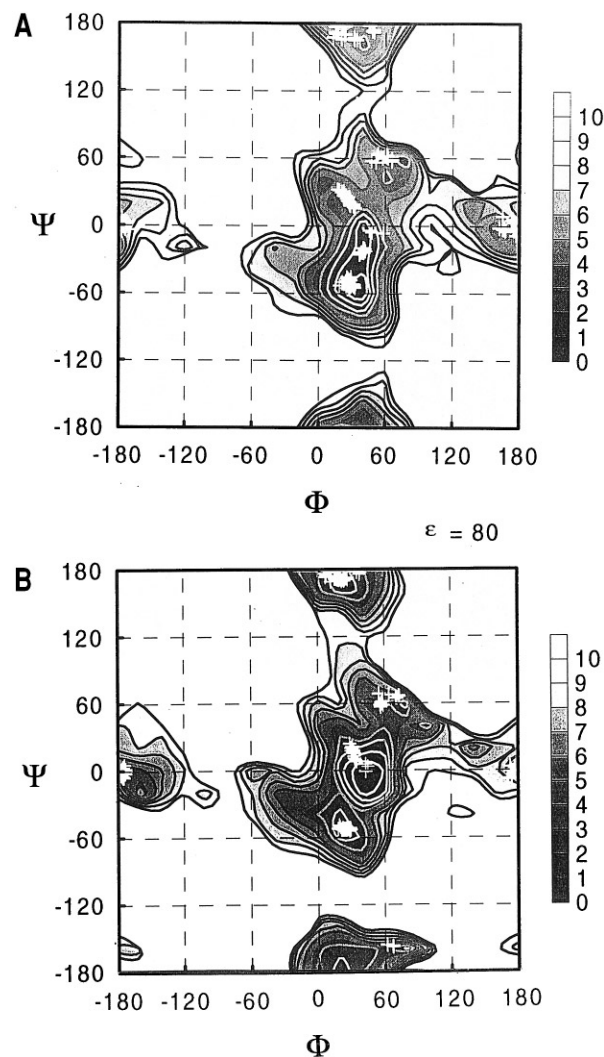

Fig. 1. RAMM calculation CCA-derived data of Galβ1-3GlcNAcβ1-R at (A) $\varepsilon = 1.5$ and (B) $\varepsilon = 80$. Energy levels were calculated from 0 to 41.86 kJ (0−10 kcal/mol); low-energy positions are marked by crosses.

lifting the grid-system-inherent constraints on the Φ/Ψ torsion angles, the energy minimisation for the disaccharide from diverse starting positions in the Φ/Ψ plane yielded families of clusters, shown by crosses in Fig. 1. They increase the accuracy of the delineation of the positions of the energy minima. As also confirmed by calculations at $\varepsilon = 4$, no pronounced shifts appeared to occur in this respect. Since the MM calculations can provide no information on the transitions of the disaccharide between the discerned minima and their population density, it is essential to complement MM analysis by MD simulations. The Φ/Ψ trajectory derived from MD simulations of Galβ1-3GlcNAcβ1-R (using CVFF with explicit consideration of solvent molecules) reveals that the main minimum reached from various starting positions was ascribed approximately to a position of a Φ/Ψ combination of one of the minima discerned by the MM methods (Fig. 2A). Evidently, no transitions to the local side minima at (180°/0°) or (20°/180°) were observed. Since this combination of different computational methods provides a detailed description of the conformational behaviour of Galβ1-3GlcNAcβ1-R, Galβ1-3GalNAcβ1-R and Galβ1-2Galβ1-R$'$ in its free state, its availability is essential to arrive at a profound interpretation of the corresponding NMR results. Therefore, this analysis had also to be performed also for Galβ1-3GalNAcβ1-R to quantitate the extent of alterations, when the epimeric position
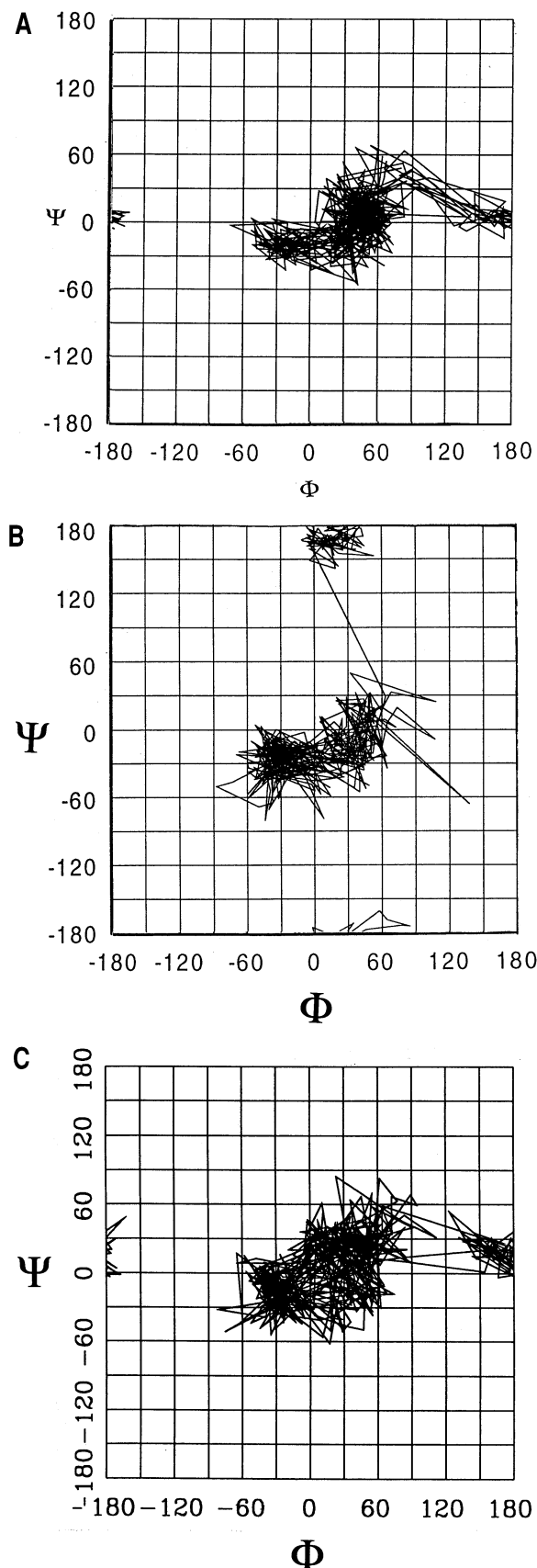
Fig. 2. MD simulation of the conformation of (A) Galβ1-3GlcNAcβ1-R, with the start coordinates of Φ,Ψ (180°/0°), (B) Galβ1-3Gal-NAcβ1-R, with the start coordinates of Φ,Ψ (0°/180°) and (C) Galβ1-2Galβ1-R′ with the start coordinates of Φ,Ψ (180°/0°) using CVFF with the explicit inclusion of solvent molecules at 300 K and a simulation time of 1000 ps.

of the 4′-OH group in the penultimate saccharide unit was changed. RAMM calculations and MD simulations of Galβ1-2Galβ1-R′ had already been described elsewhere [28]. Similar to the energy map of Galβ1-3GlcNAcβ1-R shown in Fig. 1, the calculations for Galβ1-3GalNAcβ1-R clearly pinpoint a rather shallow slope around the global energetic minimum at Φ values between 30−40° (not shown). This is also the case for Galβ1-2Galβ1-R′ [28]. The Ψ angle of Galβ1-3GlcNAcβ1-R and Galβ1-3GalNAcβ1-R adopts values at −50° and 15°, respectively. A small side minimum around (60°/60°) is also populated in the cases of Galβ1-3GlcNAcβ1-R and Galβ1-3GalNAcβ1-R. The Ψ angle of a minimum conformation of Galβ1-2Galβ1-R′ had been found to be around 30° [28].

Since various plant lectins and galectins can recognise a panel of diverse natural and synthetic disaccharides with galactose at the non-reducing terminus, it is informative to document whether these spatial parameters are influenced by the presence of the 2′-N-acetyl group commonly occurring in natural oligosaccharides. The comparison of the data for Galβ1-3Glc and Galβ1-3GlcNAc as well as for Galβ1-3Gal and Galβ1-3GalNAc after RAMM calculations and CCA disclosed no marked shift in the positions of the global and local minima caused by the presence or absence of the N-acetyl group, e.g. shown for Galβ1-3Glc (Fig. 3). Moreover, a comparison between RAMM-derived results obtained for Galβ1-3GalNAc or Galβ1-3GlcNAc and Galβ1-3GalNAcβ1-R or Galβ1-3GlcNAcβ1-R excluded that the presence of the allyl chain at the reducing end can affect the energetic distribution of Φ/Ψ-value combinations (not shown). To prove that this result is not unique as a reflection of a certain force field, other parametrisation protocols such as CHEAT, CHARMM, AMBER and GROMOS were similarly applied. These calculation sets led to similar results and thus enhanced the level of credibility of the data obtained.

To provide a similar basis of calculation-derived parameters for the three ligands to be tested in binding assays MD analysis of Galβ1-3GalNAcβ1-R and Galβ1-2Galβ1-R′ (Fig. 2B, C) demonstrated a conformational flexibility comparable to that of Galβ1-3GlcNAcβ1-R (Fig. 2A). The epimeric change of the 4′-OH group of the unit at the reducing end thus fails to exert a notable effect on the conformational behaviour. The MD simulations were performed at a simulation temperature of 300 K in line with the conditions of the NMR experiments. To exclude the presence of additional side minima, simulations at a temperature of 400 K were also performed. No transitions into different side minima were observed. To test the overall importance of the global minimum MD simulations were started from two additional combinations of (Φ/Ψ) pairs which are not positioned within the detected minima or their vicinity, i.e. (180°/0°) and (0°/180°). Transitions to the determined minima occurred after a few picoseconds (not shown). These calculations define a certain set of theoretically feasible conformations. Their actual value depends on the support by experimental data, obtained by NMR measurements.

NMR study of conformational aspects of the disaccharide ligands. Galβ1-3GlcNAcβ1-R, Galβ1-3GalNAcβ1-R and Galβ1-2Galβ1-R′ were subjected to rigorous assignment of the ¹H and ¹³C chemical shifts recorded at 500 and 125 MHz (Table 1). Assignments were based on COSY, RCT, TOCSY and HMQC experiments. To evaluate the validity of the calculated conformational parameters, the information of the NOE and ROE experiments is pertinent. An interresidual distance of 2.4 Å (between two protons of different residues) was detected for Galβ1-3GlcNAcβ1-R due to a magnetisation energy transfer from Gal H1 to GlcNAc H3 and *vice versa*. Additionally, an interresidual contact between Gal H1 and GlcNAc H2 was measured whose
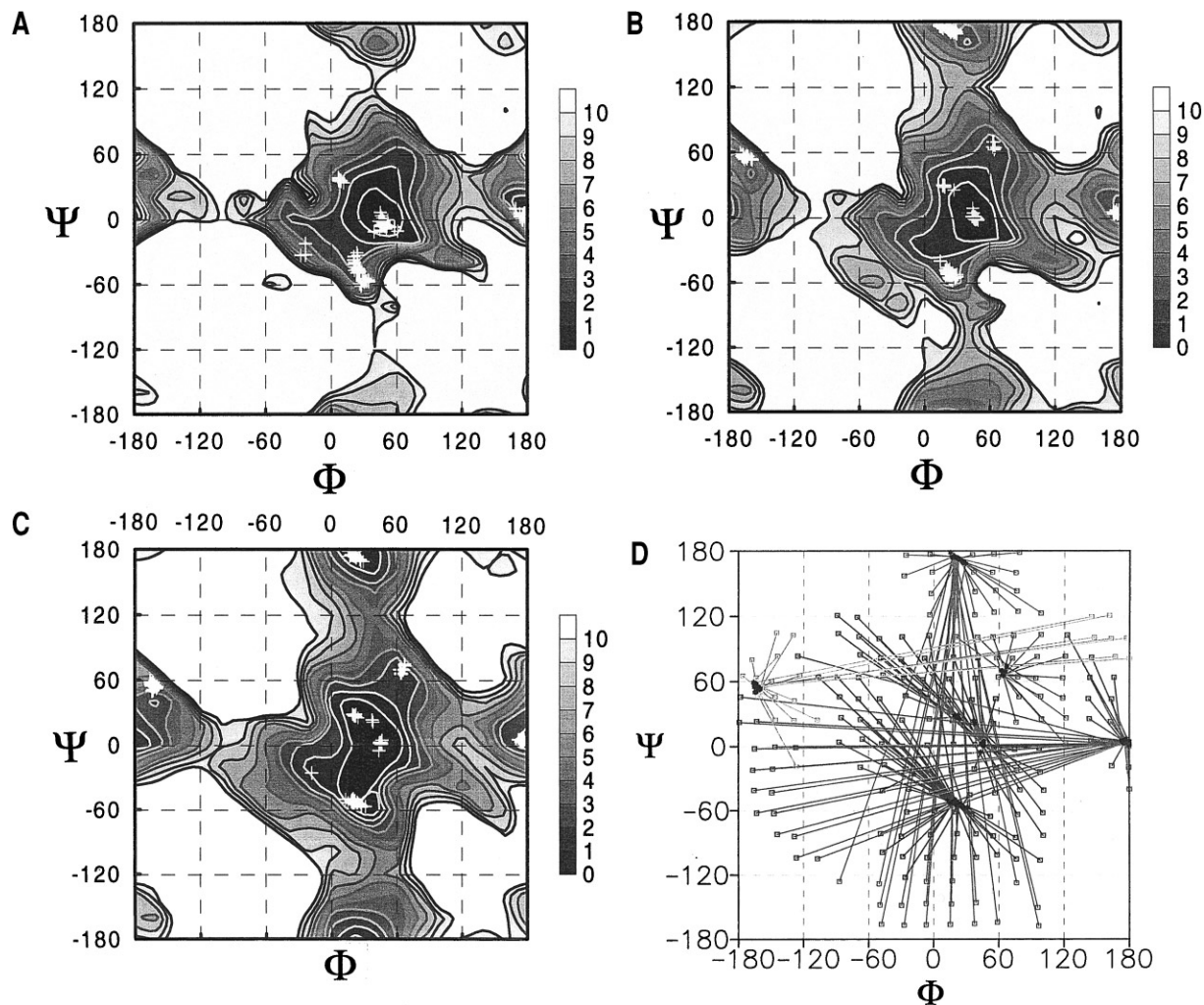
Fig. 3. RAMM calculations and CCA-derived data on conformational aspects of Galβ1-3Glc at (A) ε = 1.5, (B) ε = 4 and (C) ε = 80 as well as (D) illustrates of CCA plot of Galβ1-3Glc at ε = 80. Energy levels were calculated from 0 to 41.86 kJ (0−10 kcal/mol); low-energy positions are marked by crosses.

Table 1. Compilation of the chemical shifts of ¹H and ¹³C signals for Galβ1-3GlcNAcβ1-R, Galβ1-3GalNAcβ1-R and Galβ1-2Galβ1-R′.

Saccharide	Atom	Chemical shift at position					
		1	2	3	4	5	6/6′
		ppm					
Galβ1-3GlcNAcβ1-R	Gal H	4.42	3.52	3.64	3.91	3.71	3.75/3.78
	Gal C	104.70	71.86	73.66	69.72	76.47	62.19
	GlcNAc H	4.60	3.86	3.78	3.55	3.48	3.93/3.78
	GlcNAc C	101.00	55.69	83.69	69.91	76.59	61.91
Galβ1-3GalNAcβ1-R	Gal H	4.43	3.52	3.61	3.90	3.66	3.79/3.75
	Gal C	106.20	71.89	73.79	69.93	76.32	62.26
	GalNAc H	4.55	4.02	3.86	4.18	3.70	3.79/3.75
	GalNAc C	101.53	52.48	81.29	69.23	76.18	62.26
Galβ1-2Galβ1-R′	Gal′ H	4.74	3.61	3.72	3.96	3.73	3.79/3.80
	Gal′ C	106.28	74.28	75.17	71.31	77.84	63.55
	Gal H	4.55	3.79	3.89	3.97	3.73	3.79/3.80
	Gal C	103.99	81.65	75.56	71.31	77.84	63.55

recorded intensity translated into a distance of 2.9 Å. Upper and lower limits of these average distance constraints were incorporated into a Ramachandran-type representation to derive possible Φ,Ψ torsion angle combinations about the glycosidic linkage.

The distance map of Galβ1-3GlcNAcβ1-R with the two NOE-derived constraints based on the two interresidual contacts in the free state is given in Fig. 4. Since there is no area of overlap, it is a reasonable explanation that at least two conformations of
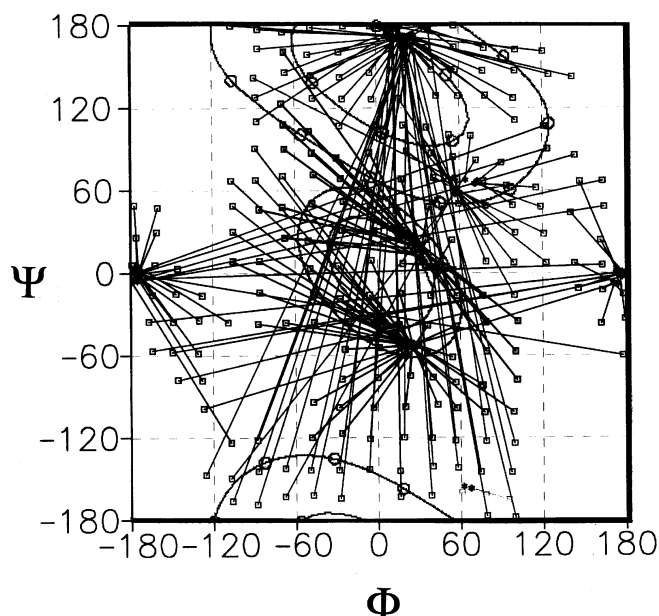
Fig. 4. Distance map of Galβ1-3GlcNAcβ1-R in the free state in combination with CCA-derived data at ε = 80.
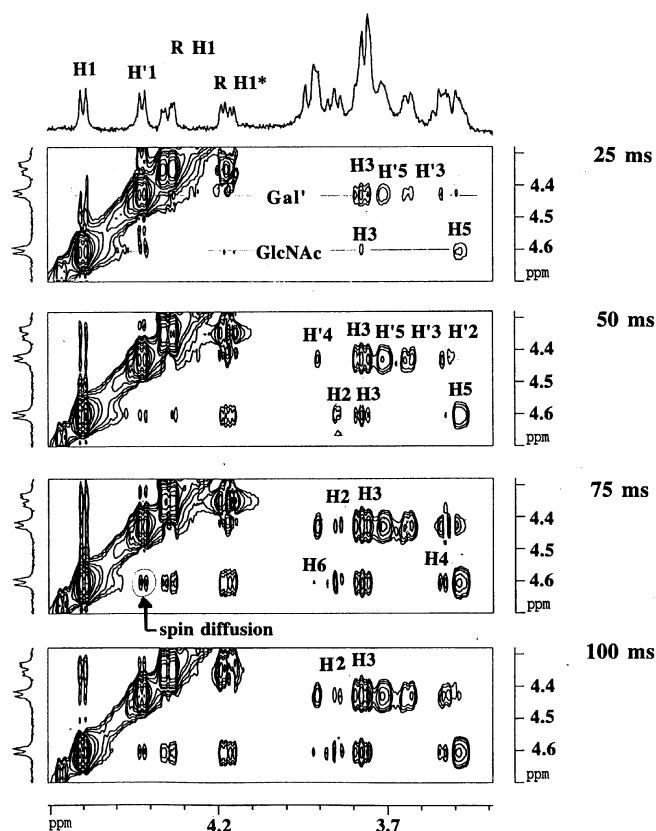

Fig. 5. Relevant section of a 2D NOESY spectrum of Galβ1-3GlcNAcβ1-R in the presence of the galactoside-specific mistletoe lectin. The ligand/lectin ratio was 10:1 and the spectrum was recorded at 500 MHz ^{1}H frequency and 298 K with mixing times of 25, 50, 75 and 100 ms.

Fig. 6. TRNOE-derived distance map of Galβ1-3GlcNAcβ1-R in complex with the galactoside-specific mistletoe lectin, based on the two measured interresidual NOE contacts. (○——○) Gal H1-GlcNAc H3, 2.2 Å (lower limit, van der Waals' distance), 2.5 Å (upper limit, measured NOE distance); (– – –) Gal H1−GlcNAc H2, 2.2 Å, 3.2 Å. The area of overlap in the Φ/Ψ diagram defines the permissible set of angle combinations in which both constraints are satisfied in one conformation. Superposition of the distance map of Galβ1-3GlcNAcβ1-R in complex with the galactoside-specific mistletoe lectin and the RAMM-derived energy profile of the same disaccharide in the free state at ε = 1.5.

harbour clusters of low-energy conformations yielded by CCA. Therefore, conformational clustering data obtained for two different dielectric constants were implemented into this distance map; an example is shown for ε = 80 (Fig. 4). It is obvious that the clusters are located in the two sets of Φ,Ψ combinations corresponding to the NOE-derived interresidual distances except for the combination (180°/0°). This result argues in favour of different well-defined conformations which contribute to the time- and ensemble-averaged NOE data. Having thus defined the free-state conformations of the first ligand, NMR data of Galβ1-3GalNAcβ1-R were collected and led to assessment of only one interresidual NOE contact between Gal H1 and GalNAc H3. Together with the results from the RAMM-derived energy maps, it is reasonable to conclude that the free-state conformation of Galβ1-3GalNAcβ1-R can be rather similar to that of Galβ1-3GlcNAcβ1-R. As already mentioned, conformational information on Galβ1-2Galβ1-R′, in addition to Fig. 2C, has already been presented [28]. The next step of our investigation addressed the question whether lectin binding will affect torsion angles of the glycosidic linkage.

Analysis of ligand conformations in the complex. Differences in the line widths between proton signals of the protein and the disaccharide derivatives could readily allow one to discern the origin of the signals. Indeed, the one-dimensional (1D) ^{1}H-NMR spectrum of the B chain (34 kDa) of VAA at millimolar concentration showed fairly broad and unresolved signals. It is therefore easy to distinguish the signals of the lectin from those of the ligand. TRNOE spectra were recorded with the hololectin and the purified galactoside-binding B chain. No measurable influence of the A chain was seen within the comparative sets of experiments (not shown). To define the optimal conditions to acquire meaningful TRNOE data, different sets of parameters such as temperature and ligand/protein ratio were systematically varied at 360 MHz. In order to increase resolution and sensitivity, the 1D and 2D TRNOE experiments were performed at

Galβ1-3GlcNAcβ1-R are present in the free state. Evidently, the two different interresidual NOE distances cannot be accommodated in a single conformation. In this case, it should be expected that the two NOE-defined portions of the Φ,Ψ space will
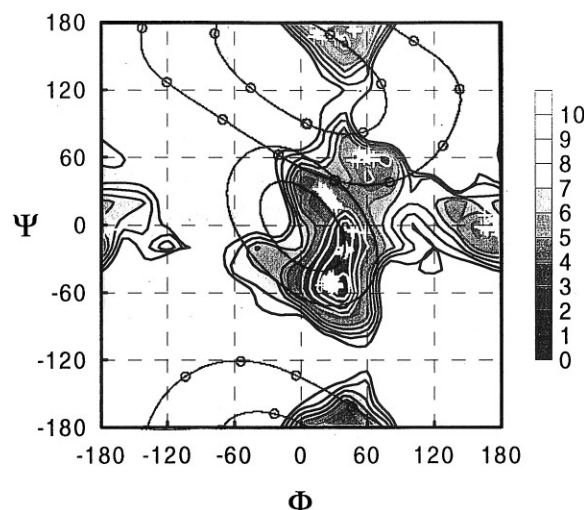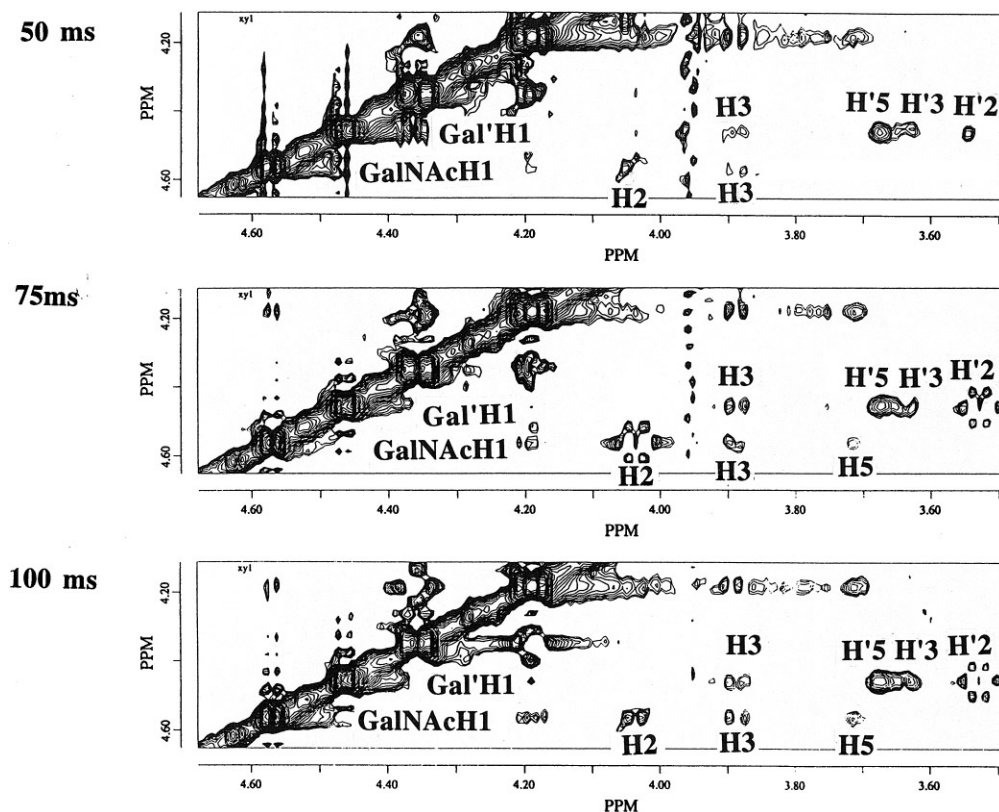
Fig. 7. Relevant part of a 2D NOESY spectrum of Galβ1-3GalNAcβ1-R in the presence of the galactoside-specific mistletoe lectin. The ligand/lectin ratio was 10:1 and the spectrum was recorded at 500 MHz ^{1}H frequency and 298 K with mixing times of 50, 75 and 100 ms.

500 MHz under optimised conditions. Different mixing times (25 ms, 50 ms, 75 ms, 100 ms) were applied in order to identify contacts originating from spin diffusion. Furthermore, ROE experiments were included to assure the focus of the interpretation on interproton contact-dependent signals exclusively of the ligand in the complex. NOE experiments were performed before and after ligand addition to correlate the measurable NOE signals of the disaccharides with the TRNOE signals occurring in different phase. As shown in the relevant parts of the NOE spectra which were recorded at different mixing times in Fig. 5, Gal H1 was spatially correlated with GlcNAc H3 and with GlcNAc H2. Gal H1 exhibited a well-defined intraresidual NOE contact with Gal H3 whose intensity is equivalent to a distance of 2.5 Å and could be used for calibration. The correlation between Gal H1 and H5, which is apparent at 75 ms, was less intense than the Gal H1/GlcNAc H2 cross-peak (Fig. 5). The calculated average interresidual distance between Gal H1 and GlcNAc H2 is 3.2 Å. The additional contact between Gal H1 and GlcNAc H1 was identified as originating from spin-diffusion effects. The TRNOE signals were transformed by integrating and comparing cross-peak volumes of NOEs into intra- and inter-residual distances. The signals were normalised with reference to diagonal cross-peak volumes. The cross-peaks involving the anomeric protons in the 2D NOESY spectra obtained at four different mixing times (25 ms, 50 ms, 75 ms, 100 ms) showed the enhancement of signal intensity; an example is presented in Fig. 5. Since the NOE signals observed for the disaccharide in the presence of VAA were negative and spin-diffusion effects were excluded, the transferred NOE signals could be reliably used to establish a distance map to delineate Φ/Ψ combinations of the bound ligand. Remarkably, an overlap of the two sets of lines was observable in the distance map of bound Galβ1-3GlcNAcβ1-R (Fig. 6). It should be recalled that no overlap was seen in the free ligand (Fig. 4).
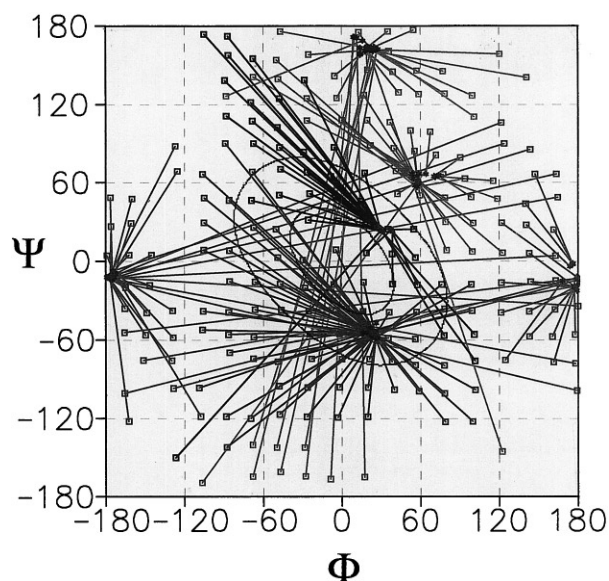

Fig. 8. TRNOE-derived distance map of Galβ1-3GalNAcβ1-R in the VAA-bound state in combination with CCA-derived data at $\varepsilon = 80$. One interresidual NOE distance was obtained: Gal H1−GlcNAc H3 = 2.2 Å (lower limit, van der Waals' distance), 2.6 Å (upper limit, measured NOE distance).

The two sets of contour lines of the distance map, shown in Fig. 6, had two points of intersection, namely at $\Phi_1/\Psi_1 = (-30°/70°)$ and $\Phi_2/\Psi_2 = (30°/40°)$. As a consequence of the RAMM calculations extended by CCA and the MD simulations, it is reasonable to assume that a possible bound-state conformation can be estimated at the second point of intersection at $\Phi_2/$
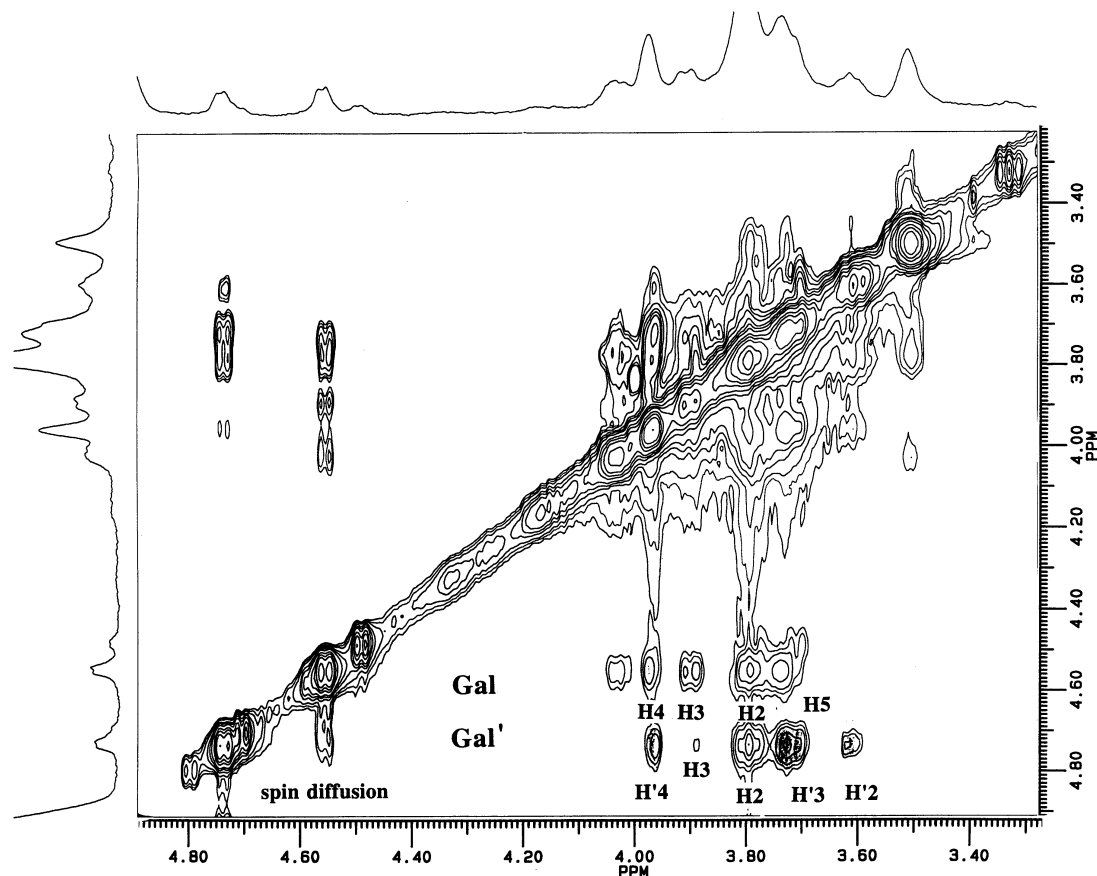
Fig. 9. 2D NOESY spectrum of Galβ1-2Galβ1-R′ in the presence of the galactoside-specific mistletoe lectin. The ligand/lectin ratio was 10:1 and the spectrum was recorded at 500 MHz ^{1}H frequency and 298 K with a mixing time of 100 ms.

Ψ_2 = (30°/40°). In this case Galβ1-3GlcNAcβ1-R complexed with mistletoe lectin can adopt a conformation which is in the vicinity of a local-minimum conformation of the free state around Φ/Ψ = (40°/15°) according to RAMM calculations shifted evidently closer by CCA (Fig. 6). Since the low-energy valley around the Φ/Ψ combination (40°/15°) is rather flat and the corresponding conformational cluster also points towards the direction of Φ_2/Ψ_2 = (30°/40°), the change in the glycosidic angles Φ and Ψ occurring after adoption of the bound state is not marked. It has to be emphasised that the local minimum around Φ/Ψ = (40°/0°) in the range of the dielectric constants between ε = 4 and ε = 80 was rather densely populated (75−90% of the whole population of the free disaccharide) and can under these conditions be referred to as the global one.

In the case of Galβ1-3GalNAcβ1-R complexed with VAA it was only possible to detect one interresidual NOE contact (Fig. 7). The interresidual distance of the two protons at the glycosidic linkage Gal H1 and GalNAc H3 was determined to be 2.6 Å. It is therefore not possible to reach reliable conclusions similar to those obtained for the other two disaccharides. However, the corresponding distance map, which is superimposed with CCA data (Fig. 8), argues in favour of presence of a *syn*-state and not an *anti*-state conformation when this disaccharide is bound to the mistletoe lectin. Furthermore, it has to be emphasised that differences between the build-up curves of both units of Galβ1-3GalNAcβ1-R, i.e. deviations in the signal intensity of NOE cross-peaks measured for the residues, revealed disparities in the strength of association of the two hexopyranose units to the lectin, as indicated in Figs 5 and 7. The faster transverse relaxation of the bound ligand raised evidence for a higher extent of immobilisation of the Gal residue in comparison to the
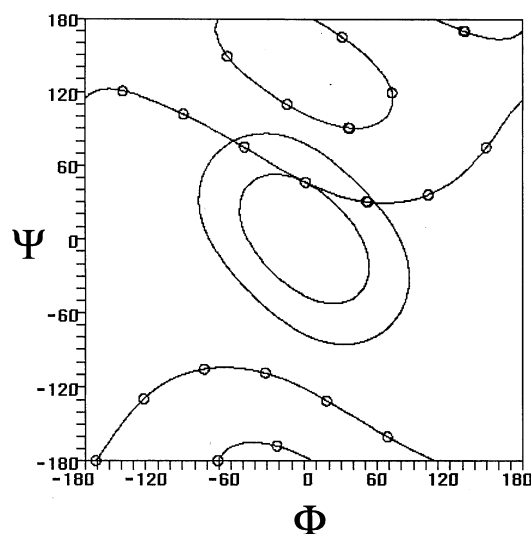

Fig. 10. TRNOE-derived distance map of Galβ1-2Galβ1-R′ in complex with the galactoside-specific mistletoe lectin, based on the two measured interresidual NOE contacts. (O———O) Gal′ H1−Gal H3, 2.3 Å (lower limit), 2.7 Å (upper limit, measured NOE distance); (− − −) Gal′ H1−Gal H2, 2.0 Å, 3.4 Å. The area of overlap in the Φ/Ψ diagram defines the set of angle combinations in which both constraints are satisfied in one conformation.

more mobile GalNAc residue at the reducing end. The NOE build-up curves of Galβ1-3GalNAcβ1-R which had been derived from the TRNOE experiments documented in Fig. 7 and the weak intensity of all intraresidual NOEs derived from the Gal-
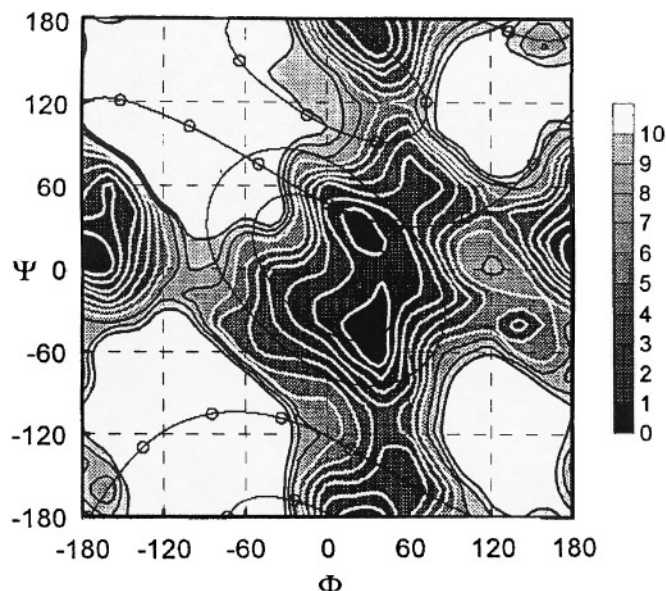
Fig. 11. Superposition of the distance map of Galβ1-2Galβ1-R′ in complex with the galactoside-specific mistletoe lectin and the RAMM-derived energy profile of the same disaccharide in the free state at ε = 4. Energy levels were calculated from 0 to 41.86 kJ, (0−10 kcal/mol).

NAc moiety, likewise seen in Fig. 7, clearly uncovered a heightened extent of mobility of the penultimate sugar unit in comparison to those of Galβ1-3GlcNAcβ1-R and Galβ1-2Galβ1-R′ when complexed to VAA. For Galβ1-3GlcNAcβ1-R/VAA and Galβ1-2Galβ1-R′/VAA complexes both hexopyranose units apparently lacked the extent of mobility observed in case of the penultimate residue of Galβ1-3GalNAcβ1-R/VAA. When Galβ1-2Galβ1-R′/VAA complexes were analysed, two interresidual contacts were observed, namely Gal′ H1−Gal H2 = 2.7 Å and Gal′ H1−Gal H3 = 3.4 Å, as shown in Fig. 9 (for discrimination we use Galβ1-2Galβ1-R′ ≙ Gal′β1-2Galβ1-R′). These two interresidual contacts led to a region of overlap in the distance map with the following points of intersection: Φ_1/Ψ_1 (−60°/80°)

and Φ_2/Ψ_2 = (60°/30°) (Fig. 10). The position of this region is different from that described for Galβ1-2Galβ1-R′ in the presence of the galectin from chicken liver [28]. The two sets of lines obtained for Galβ1-2Galβ1-R′ in complex with the mistletoe lectin encircle a region in the conformational space, which overlaps with a local energy minimum of the free state at (Φ/Ψ) = (40°/30°). This situation is graphically shown in a RAMM-derived energy profile of Galβ1-2Galβ1-R′ obtained at ε = 4 superimposed with the distance map (Fig. 11). Interestingly, the region which had been determined for the same disaccharide bound to the galectin from chicken liver [28] corresponded to the adjacent energy minimum at (30°/−60°). Thus, the plant lectin VAA and the galectin from chicken liver can apparently select different conformers of a disaccharide from solution, as compared shown Fig. 12 A and B. To underscore the validity of the assumption of conformer selection, it is pertinent to recall that both conformational states appeared to be at least in the vicinity of the populated area in MD simulation with explicit inclusion of water molecules (Fig. 2 C).

DISCUSSION

Protein−carbohydrate interaction is guided by diverse structural features which will establish the enthalpic and entropic factors leading to the measured affinity [4−10]. One aspect on the way to eventually comprehending this complex process is the precise description of the orientation of the ligand in the bound state relative to the ensemble of solution conformations and the extent of mobility of the carbohydrate units. Since lectin−ligand recognition can be involved in processes of clinical relevance such as inflammation, the NMR constraints are assumed to contribute to the development of high-affinity inhibitors for distinct lectins, as e.g. illustrated by the differential conformer selection of sialyl-Lewis[x] by E- and P-selectins versus L-selectin [43]. Using an immunomodulatory galactoside-binding plant agglutinin as a model, we have focussed here on three types of glycoligands, which are also binding partners of galectins and C-type animal lectins [26]. The typical penultimate sugar unit of β-galactosides is commonly an N-acetylated hexopyranose, leading us to study the impact of the presence of this
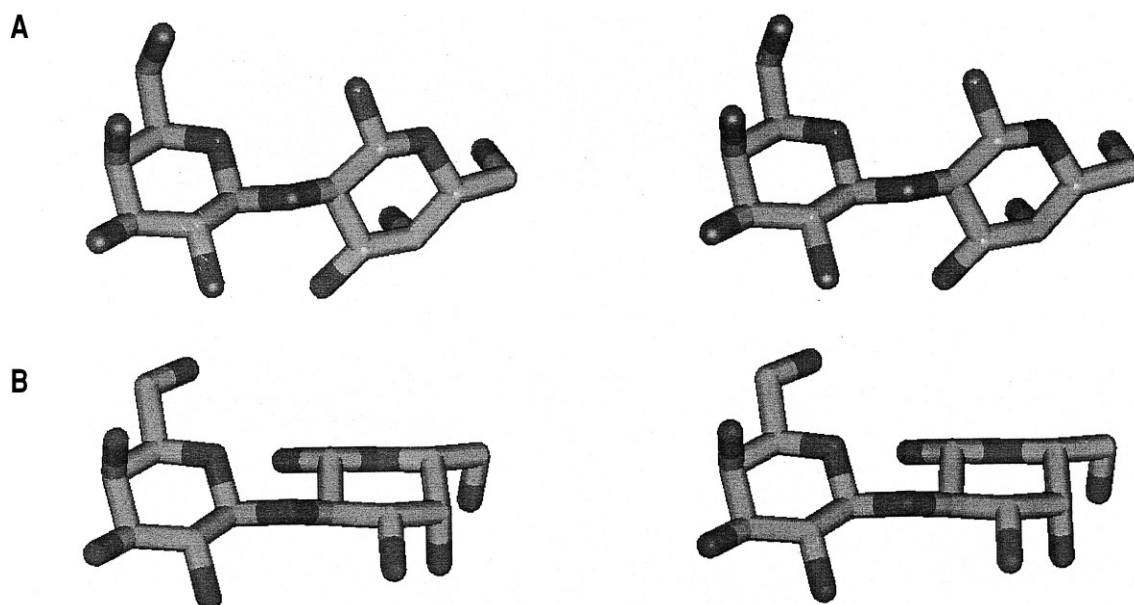

Fig. 12. Stereoplot of the low-energy Galβ1-2Galβ1-R′ conformers which are selected by different lectins, namely (A) the galactoside-specific mistletoe lectin (40°/30°) and (B) the avian liver galectin (30°/−60°).

2′-substitution. No significant conformational influence of the *N*-acetyl group was observed when comparing the data sets for Galβ1-3GlcNAcβ1-R with Galβ1-3Glcβ1-R and Galβ1-3Gal-NAcβ1-R with Galβ1-3Galβ1-R. Therefore, the difference in lectin affinity for such a pair should be caused by a direct interaction of the *N*-acetyl group with certain functional groups in the carbohydrate recognition domain of the lectin. In the case of GalNAc-terminal glycoconjugates the direct interaction with the *N*-acetyl group appears to cause a decrease of the affinity to VAA. This conclusion is in agreement with similar observations on the lack of a pronounced influence of substituents like N-glycoloyl [44] or O-acetyl [45] on the saccharide conformation.

Regarding the presented conformational data, it is remarkable that the respective results for the Galβ1-3GalNAc linkage in asialo-GM₁ and GM₁ ganglioside [46, 47] and also for the GalNAcβ1-3Gal linkage in globoside [48] show similarities with the data obtained in this study for Galβ1-3GlcNAcβ1-R and Galβ1-3GalNAcβ1-R. Glycosidic torsion angle values around (50°/0°), (25°/30°) and (30°/−40°) were found for both linkages [46−48], which are similar to the Φ,Ψ values reported herein in the RAMM/CCA-derived data sets. These values reinforce the notion that in these physiologically relevant instances the *N*-acetyl group will apparently not exert a strong impact on the spatial positioning of the glycosidic linkage. Furthermore, in these examples from the literature the conformations of the glycosidic linkages were not significantly affected by the other residues of the oligosaccharide chain.

Comparison of the conformations of Galβ1-3GlcNAc in the free state with those of the bound state indicates that one of the free-state conformations, whose relative position in the energy profile is around the global energy minimum, has evident similarities to the bound-state conformation. Due to the remaining grid-system-caused constraints in the RAMM protocol, the CCA has proved pertinent to describe more precisely Φ,Ψ angles of minimum conformations. Moreover, this technique renders the assumption rather unlikely that the conformation which is in agreement with Φ/Ψ angle pairs of the region of overlap is a virtual average conformation formed by an ensemble of different conformations. Conformer selection appears to be a reasonable explanation for the available data. In aggregate, TRNOE-experiment-derived data of Galβ1-3GlcNAcβ1-R/VAA and Galβ1-2Galβ1-R′/VAA complexes are consistent with the notion that the conformation(s) of the bound ligand represent(s) an energy minimum of the free state within the limits of accuracy of the methods used. As can be seen in the case of Galβ1-3GlcNAcβ1-R, it is possible that the bound-state conformation appears to be located at the edge of a rather flat energy minimum. It is of interest to note that observations concerning a small, but measurable change of the conformation of methyl α-lactoside after conversion to the bound state have been reported for the plant toxin ricin, still maintaining the bound ligand in the central low-energy region [49].

Besides providing information on the ligands' conformation in the complex, the analysis of build-up curves also affords access to the degree of flexibility exhibited by the penultimate sugar unit. Whereas the two mentioned disaccharides display a similar degree of mobility in the free state, this assessment points to differences in the binding strength of the terminal and the penultimate residues in the case of the Galβ1-3GalNAcβ1-R/VAA complex. Under these circumstances, the motional flexibility for the penultimate unit is apparently considerable despite ligand binding to the lectin. Although the degrees of binding affinity for Galβ1-3GlcNAcβ1-R and Galβ1-3GalNAcβ1-R had been reported to be rather similar [16, 17], the present results are in line with the assumption that the GalNAc unit has a comparatively higher extent of mobility than GlcNAc. Enthalpy-en-

tropy compensation may then cause the measurable overall affinity similarity. Precedents for motional flexibility of a penultimate sugar unit in the complex with a lectin have been reported for three plant agglutinins [50−52]. The observation that ricin accomodates the *anti*-conformation of the C-analogue of lactose [52] is a further reason why we have placed emphasis on combining calculations and experiments to provide evidence, if possible, for ligand properties of the *anti*-conformation of an O-glycoside. The notion that tight association will necessarily lead to an increased affinity can evidently not be supported, emphasising the intricate interplay of enthalpic and entropic factors which act in concert to procure complex formation. Remarkably, Galβ1-2Galβ1-R′, presenting a similar behaviour of the penultimate unit as Galβ1-3GlcNAcβ1-R, has a 10-fold higher affinity than the latter disaccharide. Since NMR-derived constraints have already been determined for this disaccharide after association to an animal lectin [28], comparison of the data sets enables one to answer the question concerning the features of the ligand in the binding site of two evolutionarily unrelated animal and plant lectins with affinity to the same ligand. Thus, we have the opportunity to decide between the possibilities of an identical or differential choice of a low-energy conformation.

When a conformer selection actually occurs, then unrelated lectins with similar nominal monosaccharide specificity should be able to bind different conformers. Since the chemical-mapping approach with tailor-made ligand derivatives has revealed differences in the binding-site topology of this plant lectin and an avian galectin [16, 53], and since we have previously described the conformational parameters of Galβ1-2Galβ1-R′ [28], the reported data for VAA now afford the opportunity to answer this question definitively, as graphically illustrated in Fig. 12.

In summary, the presented data in the individual parts of this report allow one to draw the following conclusions.

a) The experimental approach clearly shows the importance of spin diffusion in spectra of protein-carbohydrate complexes and thus strongly reinforces the necessity for adequate controls, as outlined previously [54].

b) The *N*-acetyl group has no notable impact on the conformational characteristics of the two naturally occurring β1-3-linked disaccharides with a 2′-*N*-acetyl group in the penultimate unit. Since Galβ1-3GalNAcβ1-All has an IC₅₀ value of 0.3 mM and Galβ1-3Galβ1-All has an IC₅₀ value of 0.08 mM in an asialofetuin-binding assay [16, 17], it can be concluded that the *N*-acetyl group is physically involved in reducing binding potency of the disaccharide to the lectin.

c) The detected bound-state conformations for the three disaccharides, namely Galβ1-3GalNAcβ1-R, Galβ1-3GlcNAcβ1-R and Galβ1-2Galβ1-R′, appear to be similar to certain energy-minimum conformations of the free state, adopting exclusively *syn*-state conformations.

d) The penultimate saccharide unit of Galβ1-3GalNAcβ1-R interacts rather weakly with the lectin's binding site allowing this monosaccharide residue to tumble more rapidly, yielding low-intensity intraresidual cross-peaks. Such a behaviour is not seen for Galβ1-3GlcNAcβ1-R and Galβ1-2Galβ1-R′.

e) Conformer selection in the case of Galβ1-2Galβ1-R′ is different for a galectin and a plant lectin with the same nominal monosaccharide specificity and high-level affinity to this ligand. This result substantiates the requirement for in-depth conformational analysis within studies aiming at the eventual design of synthetic ligands with superior binding capacity to a selected receptor [55−57].

REFERENCES

1. Sharon, N. & Lis, H. (1989) Lectins as cell recognition molecules, *Science 246*, 227−234.

2. Gabius, H.-J., Kayser, K. & Gabius, S. (1995) Protein-Zucker-Erkennung. Grundlagen und medizinische Anwendungen am Beispiel der Tumorlektinologie, *Naturwissenschaften 82*, 533−543.

3. Gabius, H.-J. & Gabius, S. (eds) (1997) *Glycosciences: Status and perspectives*, Chapman & Hall, Weinheim, London.

4. Carver, J. (1993) Oligosaccharides: how can flexible molecules act as signals? *Pure & Appl. Chem. 65*, 763−770.

5. Peréz, S., Imberty, A. & Carver, J. (1994) Molecular modeling: an essential component in the structure determination of oligosaccharides and polysaccharides, *Adv. Comput. Biol. 1*, 147−202.

6. Toone, E. J. (1994) Structure and energetics of protein-carbohydrate complexes, *Curr. Opin. Struct. Biol. 4*, 719−728.

7. Cambillau, C. (1995) The structural features of protein-carbohydrate interactions revealed by X-ray crystallography, in *Glycoproteins* (Montreuil, J., Vliegenthart, J. F. G. & Schachter, H., eds) pp. 29−65, Elsevier Science, Amsterdam.

8. Lemieux, R. U. (1996) How water provides the impetus for molecular recognition in aqueous solution, *Acc. Chem. Res. 29*, 373−380.

9. Bundle, D. R. (1997) Antibody-oligosaccharide interactions determined by crystallography, in *Glycosciences: Status and perspectives* (Gabius, H.-J. & Gabius, S., eds) pp. 311−331, Chapman & Hall, London, Weinheim.

10. Siebert, H.-C., von der Lieth, C.-W., Gilleron, M., Reuter, G., Wittmann, J., Vliegenthart, J. F. G. & Gabius, H.-J. (1997) Carbohydrate-protein interaction, in *Glycosciences: Status and perspectives* (Gabius, H.-J. & Gabius, S., eds) pp. 291−310, Chapman & Hall, London, Weinheim.

11. Read, R. J. & Stein, P. E. (1993) Toxins, *Curr. Opin. Struct. Biol. 3*, 853−860.

12. Barbieri, L., Batelli, M. G. & Stirpe, F. (1993) Ribosome-inactivating proteins from plants, *Biochim. Biophys. Acta 1154*, 237−282.

13. Gabius, H.-J. (1994) Lectinology meets mythology: oncological future for the mistletoe lectin? *Trends Glycosci. Glycotechnol. 6*, 229−238.

14. Gabius, H.-J., Walzel, H., Joshi, S. S., Kruip, J., Kojima, S., Gerke, V., Kratzin, H. & Gabius, S. (1992) The immunomodulatory β-galactoside-specific lectin from mistletoe: partial sequence analysis, cell and tissue binding, and impact on intracellular biosignalling of monocytic leukemia cells, *Anticancer Res. 12*, 669−676.

15. Gabius, H.-J., Gabius, S., Joshi, S. S., Koch, B., Schroeder, M., Manzke, W. M. & Westerhausen, M. (1994) From ill-defined extracts to the immunomodulatory lectin: will there be a reason for oncological application of mistletoe? *Planta Med. 60*, 2−7.

16. Lee, R. T., Gabius, H.-J. & Lee, Y. C. (1992) Ligand-binding characteristics of the major mistletoe lectin, *J. Biol. Chem. 267*, 23722−23727.

17. Lee, R. T., Gabius, H.-J. & Lee, Y. C. (1994) The sugar-combining area of galactose-specific toxic lectin of mistletoe extends beyond the terminal sugar residue: comparison with a homologous toxic lectin, ricin, *Carbohydr. Res. 254*, 269−276.

18. Gupta, D., Kaltner, H., Dong, X., Gabius, H.-J. & Brewer, C. F. (1996) Comparative cross-linking activities of lactose-specific plant and animal lectins and a natural lactose-binding immunoglobulin G fraction from human serum with asialofetuin, *Glycobiology 6*, 843−849.

19. Albrand, J. P., Birdsall, B., Feeney, J., Roberts, G. C. K. & Burgen, A. S. V. (1979) The use of transferred nuclear Overhauser effects in the study of the conformations of small molecules bound to proteins, *Int. J. Biol. Macromol. 1*, 37−41.

20. Clore, G. M. & Gronenborn, A. M. (1982) Theory and applications of the transferred nuclear Overhauser effect to the study of the conformations of small molecules bound to proteins, *J. Magn. Reson. 48*, 402−417.

21. Clore, G. M. & Gronenborn, A. M. (1983) Theory of the time-dependent transferred nuclear Overhauser effect: applications of structural analysis of ligand-protein complexes in solution, *J. Magn. Reson. 53*, 423−442.

22. Otting, G. (1993) Experimental NMR techniques for studies of protein-ligand interactions, *Curr. Opin. Struct. Biol. 3*, 760−768.

23. Ni, F. (1994) Recent developments in transferred NOE methods, *Progr. NMR Spectr. 26*, 517−606.

24. Poveda, A., Asensio, J. L., Espinosa, J. F., Martin-Pastor, M., Cañada, J. & Jiménez-Barbero, J. (1996) Applications of nuclear magnetic resonance spectroscopy and molecular modeling to the study of protein-carbohydrate interactions, *Second Electronic Glycoscience Conference (EGC-2) on the Internet and World Wide Web*.

25. Peters, T. & Pinto, B. M. (1996) Structure and dynamics of oligosaccharides: NMR and modeling studies, *Curr. Opin. Struct. Biol. 5*, 710−720.

26. Gabius, H.-J. (1997) Animal lectins, *Eur. J. Biochem. 243*, 543−576.

27. Mulder, H., Schachter, H., Thomas, J. R., Halkes, K. M., Kamerling, J. P. & Vliegenthart, J. F. G. (1996) Identification of GDP-Fuc :Galβ1-3GalNAc-R (Fuc to Gal) α1-2 fucosyltransferase and a GDP-Fuc:Galβ1-4GlcNAc (Fuc to GlcNAc) α1-3 fucosyltransferase in connective tissue of the snail *Lymanaea stagnalis, Glycoconjugate J. 13*, 107−113.

28. Siebert, H.-C., Gilleron, M., Kaltner, H., von der Lieth, C.-W., Kozár, T., Bovin, N. V., Korchagina, E. Y., Vliegenthart, J. F. G. & Gabius, H.-J. (1996) NMR-based, molecular dynamics- and random walk molecular mechanics-supported study of conformational aspects of a carbohydrate ligand (Galβ1,2Galβ1-R) for an animal galectin in the free and in the bound state, *Biochem. Biophys. Res. Commun. 219*, 205−212.

29. Bohne, A., Lang, E. & von der Lieth, C.-W. (1998) W3-SWEET: Carbohydrate Modeling by Internet, *J. Mol. Model. 4*, 33−43.

30. Grootenhuis, P. D. J. & Haasnoot, C. A. G. (1993) A CHARMm based force field for carbohydrates using the CHEAT approach: carbohydrate hydroxyl groups represented by extended atoms, *Mol. Simulat. 10*, 75−95.

31. Hagler, A. T., Huler, E. & Lifson, S. (1974) Energy functions for peptides and proteins. Deviation of a consistent force field including the hydrogen bond for amide crystals, *J. Am. Chem. Soc. 96*, 5316−5327.

32. Hagler, A. T., Lifson, S. & Dauber, P. (1979) Consistent force field studies of intermolecular forces in hydrogen-bonded crystals. 2. A benchmark for the objective comparison of alternative force fields, *J. Am. Chem. Soc. 101*, 5122−5130.

33. Weiner, S. J., Kollman, P. A., Case, D. A., Singh, U. C., Ghio, C., Alagona, G., Profeta, S. Jr & Weiner, P. (1984) A new force field for molecular mechanical simulation of nucleic acids and proteins, *J. Am. Chem. Soc. 106*, 765−784.

34. Weiner, S. J., Kollman, P. A., Nguyen, D. T. & Case, D. A. (1986) An all atom force field for simulations of proteins and nucleic acids, *J. Comput. Chem. 7*, 230−252.

35. Brooks, R. B., Bruccoleri, R. E., Olafson, B. D., States, D. J., Swaminathan, S. & Karplus, M. (1983) CHARMM: a program for macromolecular energy, minimization, and dynamics calculation, *J. Comput. Chem. 4*, 187−217.

36. van Gunsteren, W. F. (1988) The role of computer simulation techniques in protein engineering, *Protein Eng. 2*, 5−13.

37. Kozár, T., Petrak, F., Galova, Z. & Tvaroska, I. (1990) RAMM − a new procedure for theoretical conformational analysis of carbohydrates, *Carbohydr. Res. 204*, 27−36.

38. von der Lieth, C.-W., Kozár, T. & Hull, W. E. (1997) A (critical) survey of modeling protocols used to explore the conformational space of oligosaccharides, *J. Mol. Struct. 395−396*, 225−244.

39. Allinger, N. L. (1977) Conformational analysis. MM 2. A hydrogen force field utilizing V1 and V2 torsional teen, *J. Am. Chem. Soc. 99*, 8127−8134.

40. Allinger, N. L., Kok, R. A. & Imam, M. R. (1988) Hydrogen bonding in MM2, *J. Comput. Chem. 9*, 591−595.

41. Kozár, T. & von der Lieth, C.-W. (1998) Modeling conformational properties of maltose in gas phase and solvent, *Glycoconjugate J.*, in press.

42. Perlman, M. E., Davis, G. E., Koszalka, G. W., Tuttle, J. V. & London, R. E. (1994) Studies of inhibitor binding to *Escherichia coli*

purine nucleoside phosphorylase using the transferred nuclear Overhauser effect and rotating frame nuclear Overhauser enhancement, *Biochemistry 33*, 7547−7559.

43. Poppe, L., Brown, G. S., Philo, J. S., Nikrad, P. V. & Shah, B. H. (1997) Conformation of sLe^x tetrasaccharide free in solution and bound to E-, P-, and L-selectin, *J. Am. Chem. Soc. 119*, 1727−1736.

44. Siebert, H.-C., Reuter, G., Schauer, R., von der Lieth, C.-W. & Dabrowski, J. (1992) Solution conformation of GM$_3$ gangliosides containing different sialic acid residues as revealed by NOE-based distance mapping, molecular mechanics, and molecular dynamics calculations, *Biochemistry 31*, 6962−6971.

45. Siebert, H.-C., von der Lieth, C.-W., Dong, X., Reuter, G., Schauer, R., Gabius, H.-J. & Vliegenthart, J. F. G. (1996) Molecular dynamics-derived conformation and intramolecular interaction analysis of the *N*-acetyl-9-*O*-acetylneuraminic acid-containing ganglioside G$_{D1a}$ and NMR-based analysis of its binding to a human polyclonal immunoglobulin G fraction with selectivity for O-acetylated sialic acids, *Glycobiology 6*, 561−572.

46. Park, H.-J., Jhon, G.-J., Han, S. J. & Kang, Y. K. (1997) Conformational study of asialo-GM$_1$ (GA$_1$) ganglioside, *Biopolymers 42*, 19−35.

47. Acquotti, D., Poppe, L., Dabrowski, J., von der Lieth, C.-W., Sonnino, S. & Tettamanti, G. (1990) Three-dimensional structure of the oligosaccharide chain of GM$_1$ ganglioside revealed by distance-mapping procedure: a rotating and laboratory frame nuclear Overhauser enhancement investigation of native glycolipid in dimethyl sulfoxide and in water-dodecylphosphocholine solutions, *J. Am. Chem. Soc. 112*, 7772−7778.

48. Poppe, L., von der Lieth, C.-W. & Dabrowski, J. (1990) Conformation on the glycolipid globoside head group in various solvents and in the micelle-bound state, *J. Am. Chem. Soc. 112*, 7762−7771.

49. Asensio, J. L., Cañada, F. J. & Jiménez-Barbero, J. (1995) Studies of the bound conformations of methyl α-lactoside and methyl β-allolactoside to ricin B chain using transferred NOE experiments

in the laboratory and rotating frames, assisted by molecular mechanics and molecular dynamics calculations, *Eur. J. Biochem. 233*, 618−630.

50. Weimar, T. & Peters, T. (1994) *Aleuria aurantia* agglutinin recognizes multiple conformations of α-L-Fuc-(1-6)-β-D-GlcNAc-OMe, *Angew. Chem. Int. Ed. Engl. 33*, 88−91.

51. Casset, F., Hamelryck, T., Loris, R., Brisson, J.-R., Tellier, C., Dao-Thi, M.-H., Wyns, L., Poortmans, F., Pérez, S. & Imberty, A. (1995) NMR, molecular modeling, and crystallographic studies of lentil lectin-sucrose interaction, *J. Biol. Chem. 270*, 25619−25628.

52. Espinosa, J.-F., Cañada, F. J., Asensio, J. L., Dietrich, H., Martin-Lomas, M., Schmidt, R. R. & Jiménez-Barbero, J. (1996) Unterschiede zwischen den Konformationen von O- und C-Glycosiden im proteingebundenen Zustand: Ricin B, ein Galactose-bindendes Protein, erkennt unterschiedliche Konformationen von C-Lactose und dessen O-Analogon, *Angew. Chem. 108*, 323−326.

53. Solís, D., Romero, A., Kaltner, H., Gabius, H.-J. & Diaz-Mauriño, T. (1996) Different architecture of the combining sites of two chicken galectins revealed by chemical-mapping studies with synthetic ligand derivatives, *J. Biol. Chem. 271*, 12744−12748.

54. Arepalli, S. R., Glaudemans, C. P. J., Daves, G. D. Jr, Kovac, P. & Bax, A. (1995) Identification of protein-mediated indirect NOE effects in disaccharide-Fab′ complex by transferred ROESY, *J. Magn. Res. 106B*, 195−198.

55. Gabius, H.-J. (1997) Concepts of tumor lectinology, *Cancer Invest. 15*, 454−464.

56. Gabius, H.-J. (1998) The how and why of protein-carbohydrate interaction: a primer to the theoretical concept and a guide to application in drug design, *Pharm. Res. 15*, 24−31.

57. von der Lieth, C.-W., Siebert, H.-C., Kozár, T., Burchert, M., Frank, M., Gilleron, M., Kaltner, H., Kayser, G., Tajkhorshid, E., Bovin, N. V., Vliegenthart, J. F. G. & Gabius, H.-J. (1998) Lectin ligands: new insights into their conformations and their dynamic behavior and the discovery of conformer selection by lectins, *Acta Anatom.*, in the press.